

Simple One Step Synthesis of Magnetic-optical Dual Functional ZIF-8 in Sodalite Phase for Magnetically Guided Targeting Bioimaging and Drug Delivery

Sun Xujian ^{a,b,c,#}, Yang zhichao ^{a,b,c,#}, Zhang Man ^{a,b,c}, Gao Xuechuan ^{a,b,c *}

a College of Chemical Engineering, Inner Mongolia University of Technology, Hohhot 010051, China

b Key Laboratory of CO₂ Resource Utilization at Universities of Inner Mongolia Autonomous Region, Hohhot, 010051, China

c Inner Mongolia Engineering Research Center for CO₂ Capture and Utilization, Hohhot, 010051, China

Figure S1 SEM images of ZIF-8 (A, B, C)

Figure S2 SEM images of ZIF-8 (A), SEM-EDS images of ZIF-8 (B, C, D, E, F), Map Sum Spectrum of ZIF-8(G)

Figure S3 SEM-EDS images of DOX/Fe₃O₄@ZIF-8 (A, B, C, D, E, F), Map Sum Spectrum of DOX/Fe₃O₄@ZIF-8 (G)

Figure S4 (a) Raman spectra of ZIF-8; (a) Pore size distribution ZIF-8 (A) and DOX/Fe₃O₄@ZIF-8 (B)

Figure S5 (a) The TGA curves of ZIF-8 (A), DOX/Fe₃O₄@ZIF-8 (B), Fe₃O₄ (C) and DOX (D); (b) The excitation and emission spectra of DOX/Fe₃O₄@ZIF-8

Figure S6 Relaxation rate $1/T_2$ versus concentrations of Fe; T₂-weighted MRI of DOX/Fe₃O₄@ZIF-8 with diverse Fe concentrations in vitro (the inset)

Figure S7 The magnetic hysteresis loops of DOX/Fe₃O₄@ZIF-8 measured at 300 K

Figure S8 The inset shows photographs of the DOX/Fe₃O₄@ZIF-8 dispersed in water with an external magnetic field

Figure S9 Relative quantitative analysis of Dead (a), Live (b), Late apoptosis (c) and early apoptosis (d)

Figure S10 Effect of DOX/Fe₃O₄@ZIF-8 on p-JNK, p-P38, p-ERK, Caspase-3, Bcl-2, and Bax HepG2 cells were treated with DOX/Fe₃O₄@ZIF-8 for 10 min and 4 h

Figure S11 SEM images of ZIF-8 after incubation in PBS (pH = 5) at 0 (A), 1 (B), 3

(C) days and table of N, Zn, O element content in the recovered powder after incubation in PBS (pH = 5) for (0, 1, 3) days

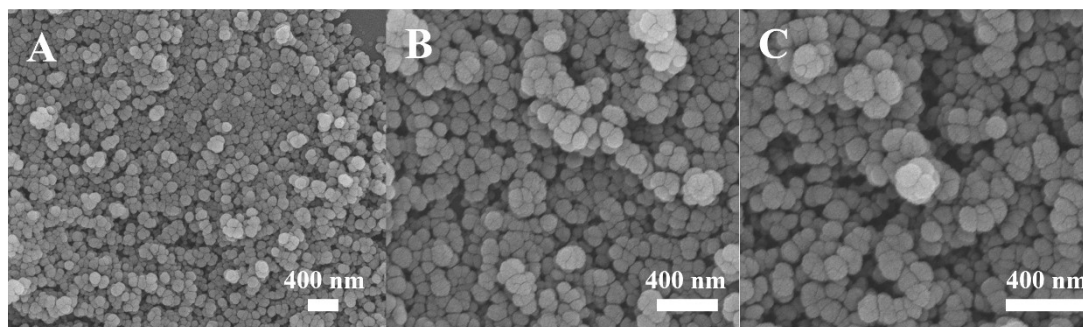


Figure S1 SEM images of ZIF-8 with different magnifications (A, B, C)

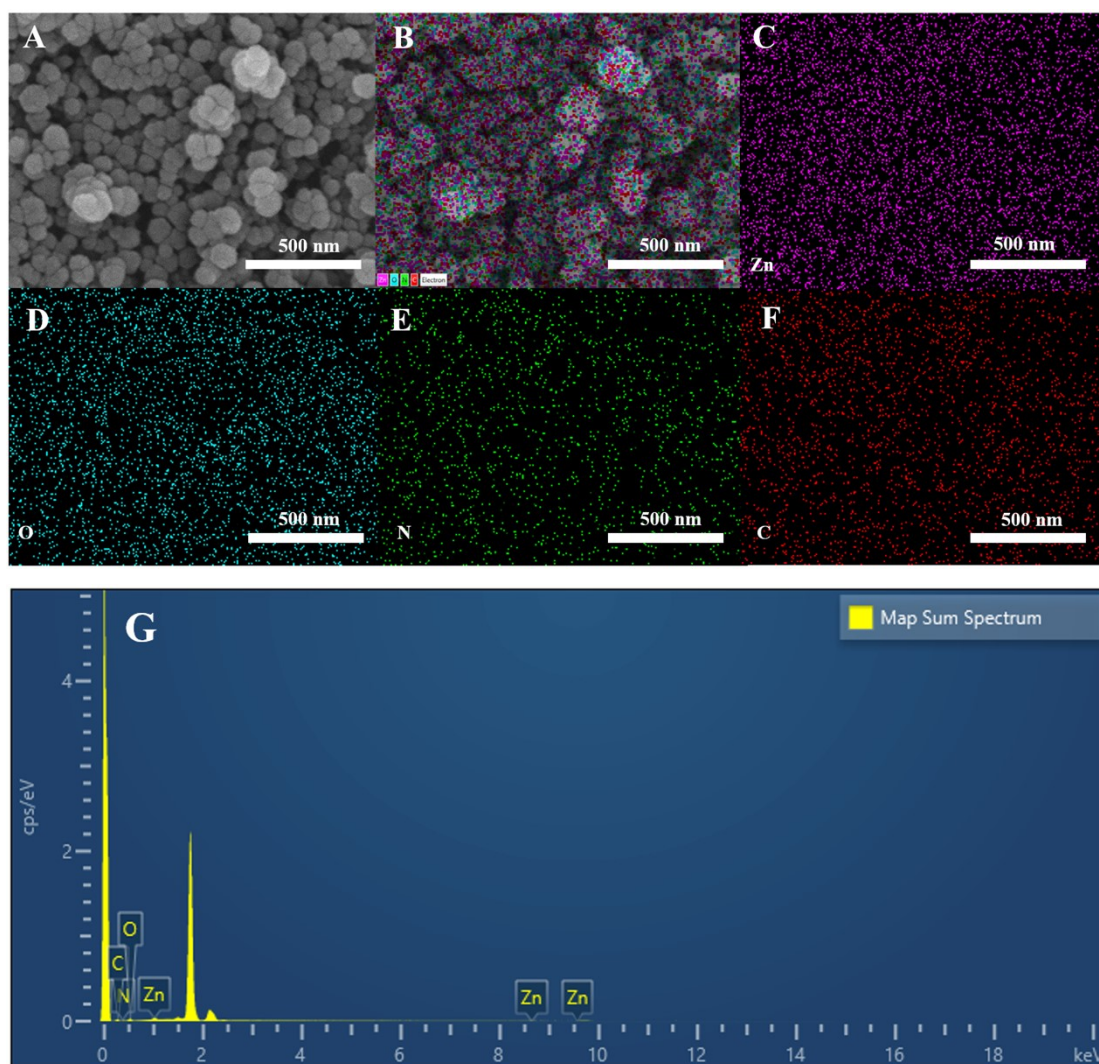


Figure S2 SEM images of ZIF-8 (A), SEM-EDS images of ZIF-8 (B, C, D, E, F), Map Sum Spectrum of ZIF-8(G)

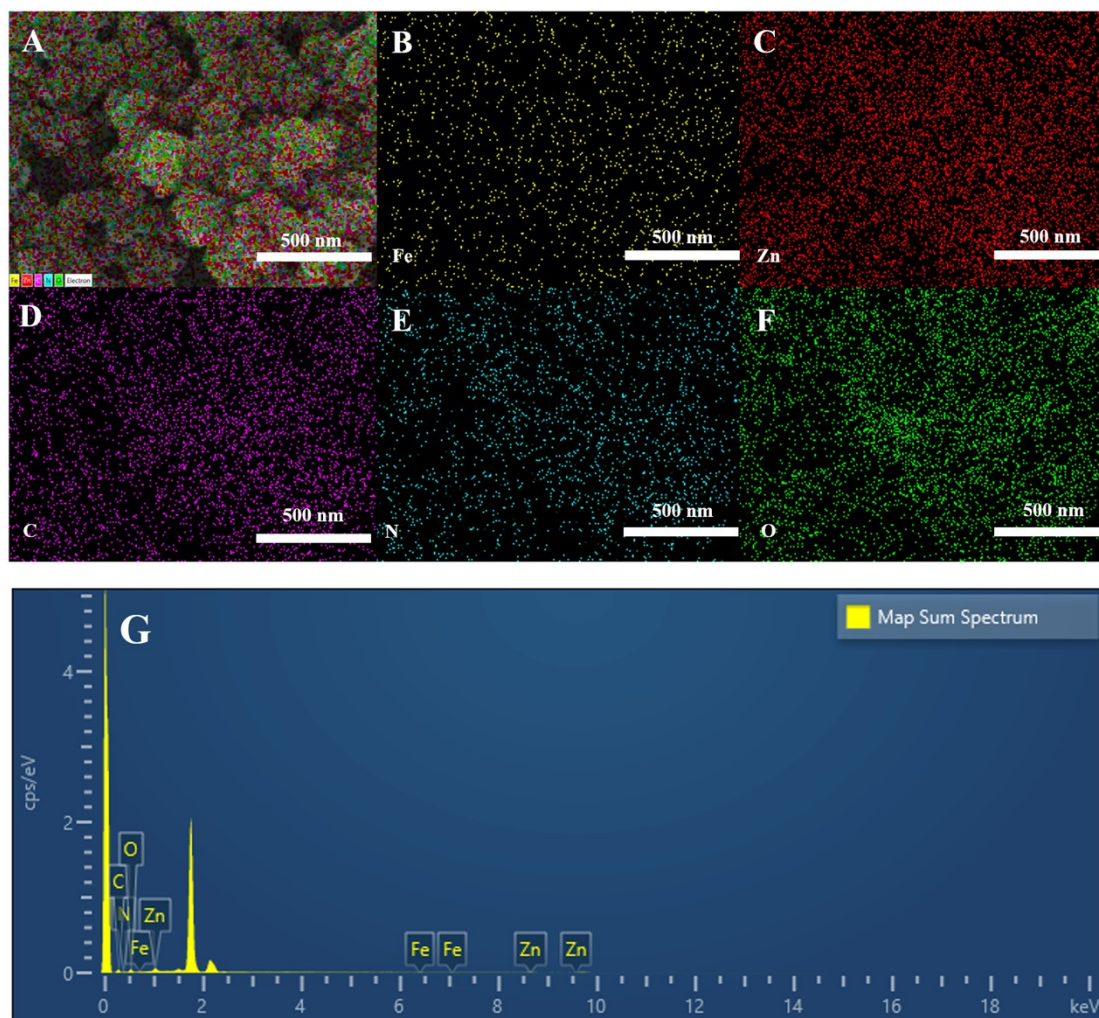


Figure S3 SEM-EDS images of DOX/Fe₃O₄@ZIF-8 (A, B, C, D, E, F), Map Sum Spectrum of DOX/Fe₃O₄@ZIF-8 (G)

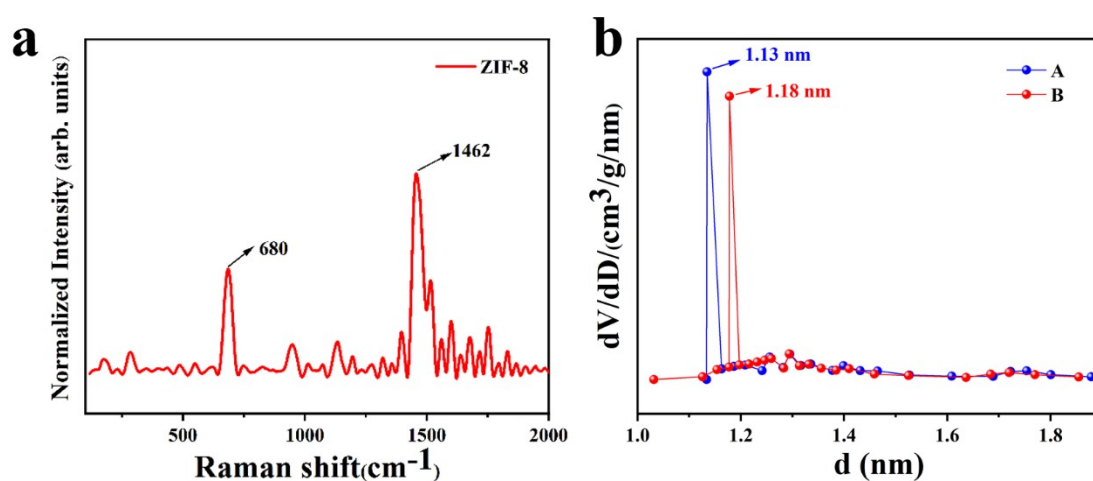


Figure S4 (a) Raman spectra of ZIF-8; (a) Pore size distribution ZIF-8 (A) and DOX/Fe₃O₄@ZIF-8 (B)

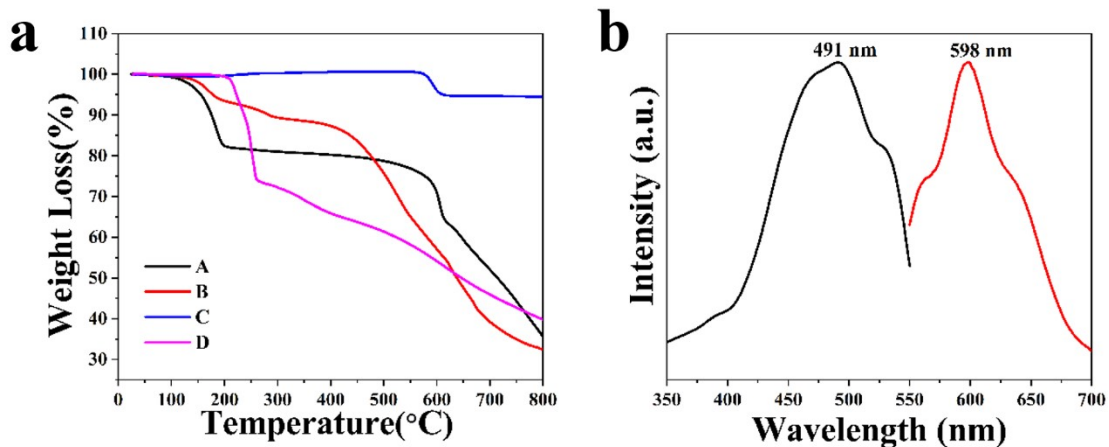


Figure S5 (a) The TGA curves of ZIF-8 (A), DOX/Fe₃O₄@ZIF-8 (B), Fe₃O₄ (C) and DOX (D); (b) The excitation and emission spectra of DOX/Fe₃O₄@ZIF-8

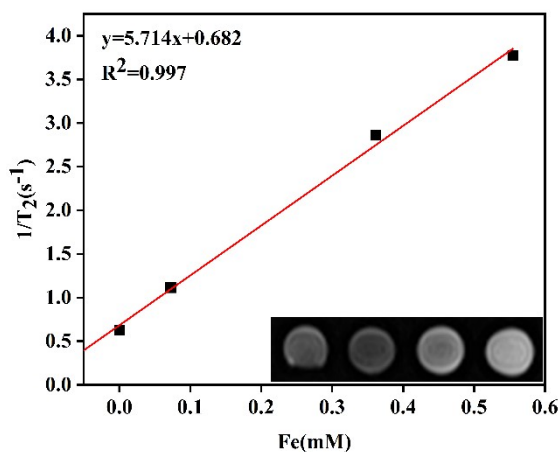


Figure S6 Relaxation rate $1/T_2$ versus concentrations of Fe. T₂-weighted MRI of DOX/Fe₃O₄@ZIF-8 with diverse Fe concentrations in vitro (the inset)

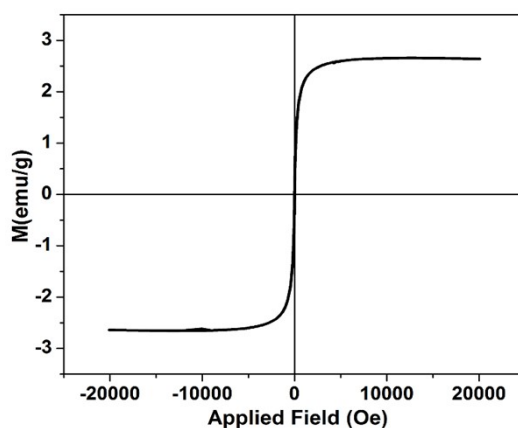


Figure S7 The magnetic hysteresis loops of DOX/Fe₃O₄@ZIF-8 measured at 300

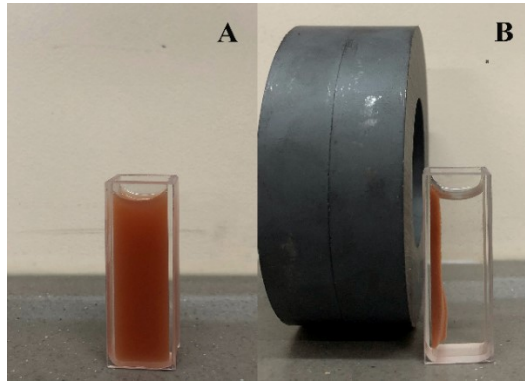


Figure S8 The inset shows photographs of the DOX/Fe₃O₄@ZIF-8 dispersed in water with an external magnetic field

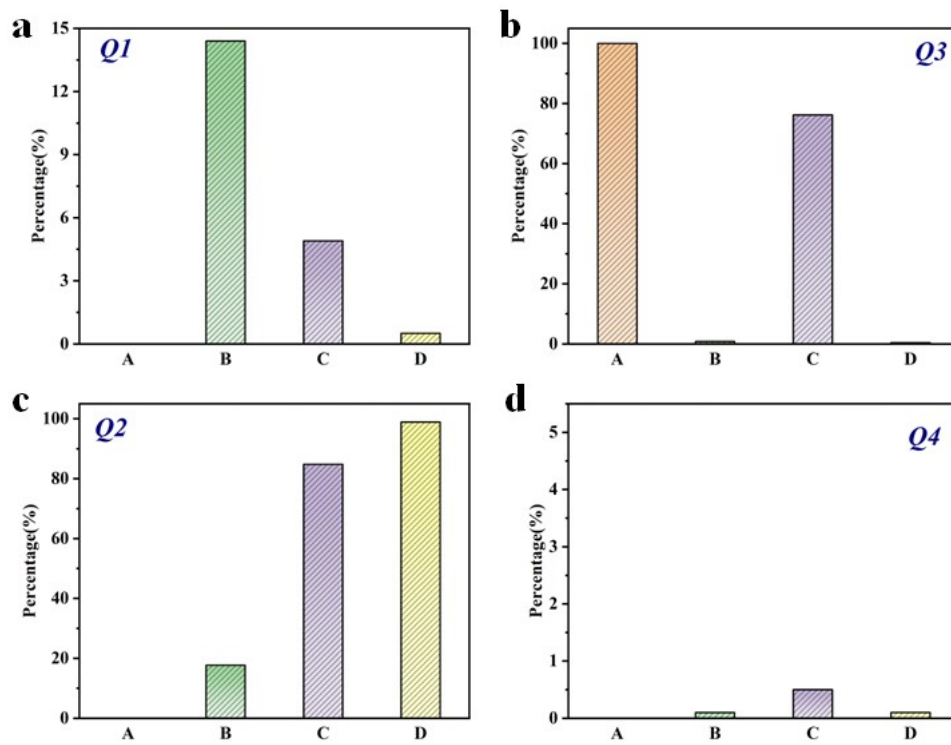


Figure S9 Relative quantitative analysis of Dead (a), Live (b), Late apoptosis (c) and early apoptosis (d)

Table S1 The percentage of Dead, Late apoptosis, Live and early apoptosis in Control, DOX, ZIF-8 and DOX/Fe₃O₄@ZIF-8

Material	Dead/Q1(Late Apop/Q	Live/Q3(Early Apop/Q
	%)	2(%)	%)	4(%)
Control	0	0	100	0
ZIF-8	3.6	17.7	78.3	0.4
DOX	4.9	18.4	76.2	0.5
DOX/Fe ₃ O ₄ @ZIF-8	0.5	98.9	0.4	0.1

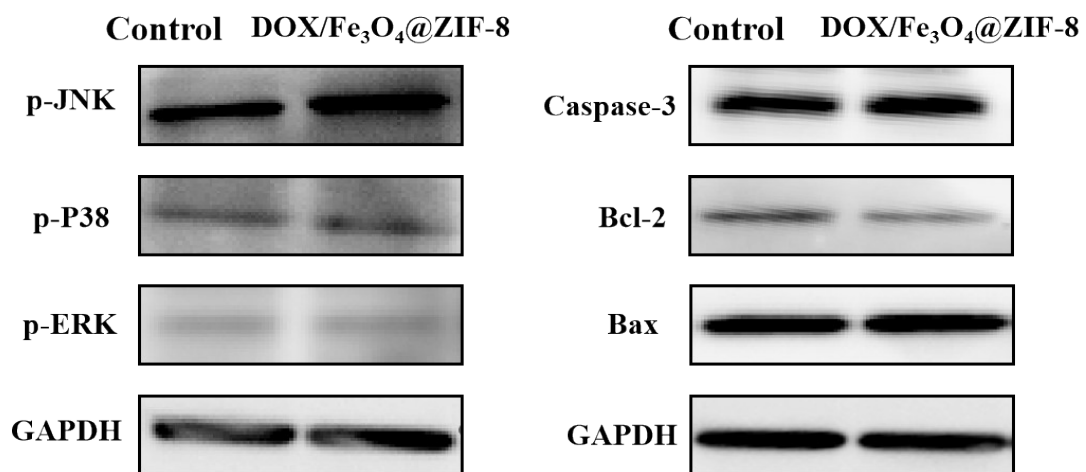
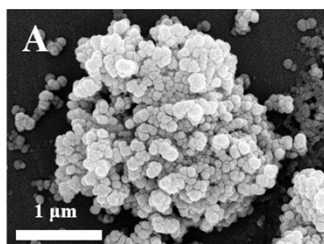
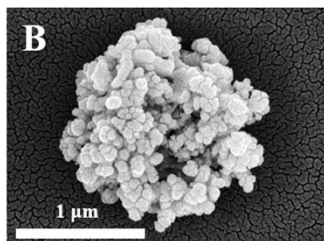


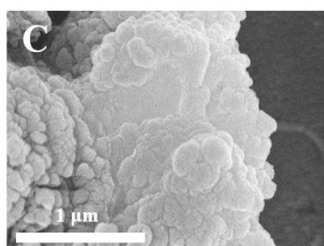
Figure S10 Effect of DOX/Fe₃O₄@ZIF-8 on p-JNK, p-P38, p-ERK, Caspase-3, Bcl-2, and Bax HepG2 cells were treated with DOX/Fe₃O₄@ZIF-8 for 10 min and 4 h



Element	Weight %
N	25.50
O	48.68
Zn	25.82



Element	Weight %
N	5.13
O	66.01
Zn	28.86



Element	Weight %
N	0.06
O	64.31
Zn	35.63

Figure S11 SEM images of ZIF-8 after incubation in PBS (pH = 5) at 0 (A), 1 (B), 3 (C) days and table of N, Zn, O element content in the recovered powder after incubation in PBS (pH = 5) for (0, 1, 3) days